Iranian Journal of Electrical and Electronic Engineering

Journal Homepage: ijeee.iust.ac.ir

Experimental Study of Charging Efficiencies and Losses of Submicron Aerosol Particles in a Cylindrical Tri-Axial Charger

P. Intra*(C.A.), P. Wanusbodeepaisarn** and T. Siri-achawawath***

Abstract: The object of the present work was to design, construct and evaluate a cylindrical tri-axial charger for charging of submicron aerosol particles by unipolar ions. The corona discharge characteristics, the intrinsic and extrinsic particle charging efficiencies, and the losses of aerosol particles were experimentally evaluated for particle diameters in the range between 50 nm and 500 nm under different operating conditions. The conditions included the corona voltages of about 7.0 to 8.0 kV, the mesh screen voltages of about 100 to 300 V and the aerosol flow rate was set at 1.5 L/min. It was found that the ion current increased from 2.90×10^{-10} to 3.66×10^{-8} A and 2.40×10^{-10} to 1.36×10^{-7} A and the number concentration of ions increased from 7.50×10^{9} to 5.92×10^{11} ions/m^3 and 6.21×10^{9} to 2.19×10^{12} ions/m^3 when the corona voltage increased from 5.5 to 8.0 kV at the mesh screen voltage between 100 and 300 V, respectively. The intrinsic charging efficiency of particles introduced a constant value of about 99% for particle diameter in the range between 50 nm and 200 nm and decreased with particle diameter in the range between about 300 nm and 500 nm at a given corona voltage. The best extrinsic charging efficiency of the studied charger occurred between 1.32% and 38% for particle diameter in the range from 50 nm to 500 nm at corona and ion trap voltages of about 7.0 kV and 300 V respectively. The highest electrostatic loss of particles was observed at 50 nm particles and it was about 89.08, 90.73 and 91.91% at a mesh screen voltage of about 300 V for corona voltages of about 7.0, 7.5 and 8.0 kV, respectively. Finally, the highest diffusion losses were at about 28.88, 23.03 and 11.15% for singly charged, neutralized and non-charged particles of 500, 500 and 50 nm, respectively.

Keywords: Aerosol, Corona Discharge, Unipolar Charging, Particle Charging.

1 Introduction

THE charging efficiency of aerosol particles is the major parameter of the aerosol charger performance [1]. It is defined as the fraction of charged particles present in the downstream portion of an aerosol charger [2]. In general for the ideal design of the aerosol charger, a charging technique for high efficiency with a high number concentration of ions and low particle losses would be needed. The most normally used method for charging of aerosol particles in the electrical aerosol instruments is the diffusion charging [3]. Depending on the polarity of the ions colliding with the particles, this method could be bipolar or unipolar. Comparing both charging methods, unipolar charging does not reach a Boltzman charge equilibrium and potentially provides a higher charging efficiency. There are three traditional techniques to produce unipolar ions for diffusion charging of aerosol particles including the corona discharge, the photoemission from

Iranian Journal of Electrical and Electronic Engineering, 2019.
Paper first received 01 December 2018 and accepted 09 January 2019.
* The author is with the Research Unit of Applied Electric Field in Engineering (RUEE), College of Integrated Science and Technology, Rajamangala University of Technology Lanna, Chiang Mai 50220, Thailand.
E-mail: panich_intra@yahoo.com.
** The author is with the Pico Innovation Co., Ltd., 336 Moo 4, Yang Noeng, Saraphi, Chiang Mai 50140, Thailand.
E-mail: paisarn@pico-innovation.com.
*** The author is with the Innovative Instrument Co., Ltd., 7/139 Bang Kaeo, Bang Phli, Samut Prakan, Bangkok 10540, Thailand.
E-mail: thanesvorn@innovative-instrument.com.
Corresponding Author: P. Intraa.

UV-light radiation, and the radiation from α-ray or β-ray sources. For the ionizing radiation, the product is a stable number concentration of ions, but the dynamic range in number concentration of ions typically is lower compared to a corona discharge [2].

Several designs of unipolar diffusion chargers both corona-wire and corona-needle for charging aerosol particles have been presented and described in published literatures [4-23]. In the corona-wire chargers, Liu *et al.* [4] was developed the corona-wire charger for evaluating the diffusion charging process of submicron aerosol particles by unipolar ions. In the Liu *et al.* [4] charger, a voltage of an alternating waveform was applied to the inner electrode to reduce the loss of particles. A modification on the Liu *et al.* [4] charger was later developed and studied by Pui [5]. From the investigation that the happening of loss of nanoparticles were associated with corona-wire chargers, Buscher *et al.* [6] modified and investigated the Pui [5] charger by applying the configuration of the metal surfaces in contact with the aerosol being entirely conductive and connected to the electrical ground, to avoid loss of particles due to insulator charging, and the inlet aerosol and sheath air tubes being modified to obtain a high penetration of particles and laminar flow in the charger. A similar design of the Pui [5] charger has also been used in the Kruis and Fissan [7] charger. In this charger, the charging region was separated from the two ion generation regions by means of metal wire screens to isolate the aerosol flow expansion into the discharge region. Biskos *et al.* [8] was later proposed and investigated the charger of Liu *et al.* [4]. In this charger, an alternating waveform voltage applied on the outer electrode driven ions to enter the charging zone without loss of charged particles on the charger walls. The inner electrode maintained a laminar flow of the aerosol stream, which was highly desirable to achieve a uniform aerosol flow. Tsai *et al.* [10] and Chien *et al.* [11-12] were designed and evaluated a multiple discharging wires charger to enhance the extrinsic unipolar charging efficiency of nanoparticles by using sheath air flow near the charger walls. Recently, a cylindrical tri-axial charger without sheath air flow was proposed and investigated by Intra [9] and was later studied for the influences of the diameter and length of corona-wire electrode on the corona discharge characteristics by Intra *et al.* [13-14]. In the corona-needle chargers, Whitby [15] was first developed the corona-needle charger which was able to converting the discharge current into unipolar ions with efficiency of about 100%. A new corona jet charger was presented by Medved *et al.* [16]. In this charger, a clean air flow transferred the free ions into the mixing chamber, and an opposing aerosol flow contributed mixing of the aerosol and the free ions. A simple corona-needle charger without sheath air capable of high efficiency charging of nanoparticles was proposed by Hernandez-Sierra *et al.* [17]. Alonso *et al.* [18] later presented a design to enhance the performance of the charger of Hernandez-Sierra *et al.* [17] by modifying the aerosol inlet geometry and the manner in which the corona-needle electrode is positioned. A similar design of the Medved *et al.* [16] charger, Park *et al.* [19] was proposed a design and performance test of a real-time unipolar charger for charging submicron particles. It was shown that the total loss of particles in the mixing and charging regions were lower than about 15%. In a later work Qi *et al.* [20] was studied the charging performance of a unipolar charger with a sonic-jet ion generator for aerosol charging. This charger eliminates the loss of the charged particles by electrostatic effect, because no electric field is included in the charging region. Recently, Intra and Tippayawong [21-23] was developed and evaluated a non-sheath air corona-needle charger. This charger demonstrated to be particularly useful as a unipolar aerosol charger, used in an electrostatic particulate matter monitor.

However, the charged particle losses due to diffusion motion and electrostatic precipitation are often severe, and require to be focused in the improvement of unipolar diffusion chargers [2]. Some of this reduction could be obtained by bring the surrounding sheath air flow at the boundary between the aerosol flow and the charger wall. It allows more space for the charged particles to flow through the charger without collecting on the charger walls. However, the high sheath air flow results in the aerosol dilution. Another method uses a turbulent jet flow of unipolar ions in a mixing chamber and applies an alternating wave voltage to the electrode instead of a DC voltage. But the mixing chamber again dilutes aerosol and the alternating wave voltage power supply are expensive and complex to use. In our previous work, Intra [9] was developed and investigated the cylindrical tri-axial charger without sheath air flow along the charger walls for diffusion charging of submicron aerosol particles by unipolar ions. It has low diffusion and electrostatic losses due to the short column charging zone (22 mm in length), and is a low cost and low complexity system. It worked as well as more complicated and expensive commercially available chargers. Recently, the corona-wire diameter and length effects on the electrostatic discharge characteristics of the cylindrical tri-axial charger were studied by Intra *et al.* [13-14]. It was showed that both positive and negative currents were decreased with increasing the wire diameter and were increased with increasing the wire length at the same ion-driving and corona voltages. However, the experimental study of the intrinsic and extrinsic charging efficiencies and the aerosol particle losses in the cylindrical tri-axial charger was not studied in detail in our previous work.

Therefore, the unipolar cylindrical tri-axial charger for diffusion charging of submicron aerosol particles was designed, constructed and experimentally investigated in this study. For economic and ease of operation reasons its design, fabrication and testing was kept

uncomplicated. The electrostatic discharge characteristics, the intrinsic and extrinsic charging efficiencies and the aerosol particle losses were experimentally evaluated for particle diameter in the range between 50 nm and 500 nm, under different operating conditions that included corona voltages of about 7.0 to 8.0 kV, mesh screen voltages of about 100 to 300 V and aerosol flow rates of about 1.5 L/min.

2 Description of Cylindrical Tri-Axial Charger

The objective of the present work was to develop a simple, compact, low cost unipolar tri-axial charger with robust operation, no dilution and sheath air flow and easy to fabricate. It capable of operating lower aerosol flow rate and lower ion current and voltage in order to reduce the energy consumption while keeping a high charging efficiency for submicron aerosol particles, making the particle charger of the electrical aerosol instruments better suited for application of the general airborne particulate monitoring. In the present charger, its developed geometrical configuration is similar to that in the Intra [9] charger. Fig. 1 shows the schematic drawing of the Intra [9] charger and the present charger. However, the following are differences between the charger by Intra [9] and the present charger; (i) to assure uniform aerosol flow distribution across the annular entrance to the charging zone of the charger, the sharp geometry of the aerosol inlet and outlet flow guides and the short column charging zone were introduced in order to eliminate the losses of the charged particle by diffusion motion and electrostatic collecting on the inner and outer electrodes of the charger; (ii) the corona-wire electrode in the ion production zone of the charger was modified by a reduction of the corona-wire diameter of about 100 µm and an increment of its length of about 22 mm to assure a uniform electric field and stabilize discharge current in order to achieve a high ion concentration in the ion production zone and a high penetration of ions over the mesh screen openings on the inner cylinder to the charging zone of the charger; and (iii) it is a simple and low cost system, its design was kept uncomplicated for economic and ease of operation reasons. The length and diameter of the prototype tri-axial charger was 126 mm and 67 mm, respectively. The comparison of different corona aerosol chargers in terms of the geometrical configuration of electrodes, the charging zone length, the aerosol and sheath air flow rates and the corona voltage range was shown in Table 1.

As shown in Fig. 1(b), it consisted of coaxial cylinders with a corona-wire electrode placed along the axis of the inner and outer cylinders. In the present charger, a diameter and length of the corona-wire electrode was about 100 µm and about 22 mm, respectively. The inner and outer cylinders were fabricated using stainless steel because it is electrically conductive, inert, corrosion resistant and very hard, and resistant to scratching. To avoid the electric field distortion due to small surface

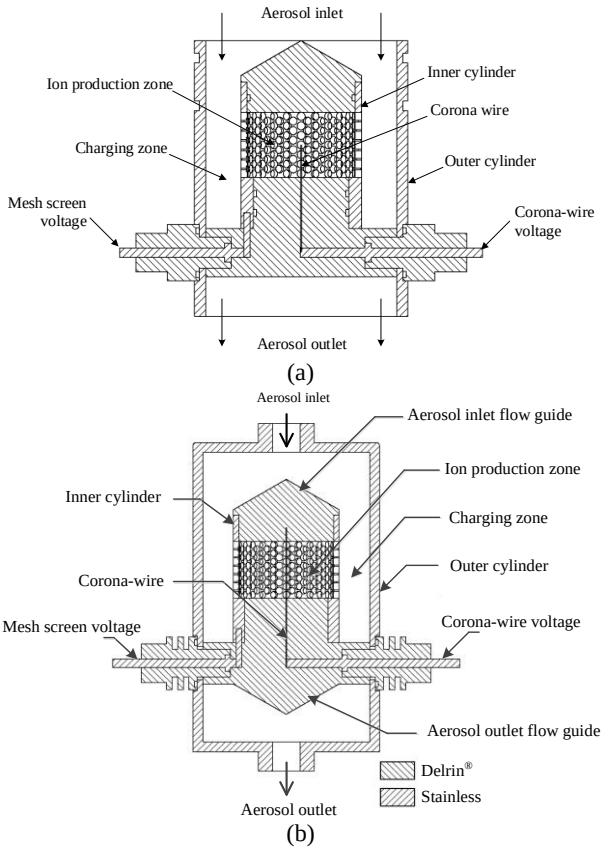

Fig. 1 Schematic diagram of a) charger by Intra [9] and b) studied charger.

scratches and imperfections, these were polished by the high precision polishing machine to an extremely fine surface complete. The inner and outer radii of the annular charging zone were about 17 mm and about 30 mm, respectively. The electrical insulation was provided by a Delrin spacer between the inner and outer cylinders, and the aerosol flowed through the space between the cylinders. A DC high voltage was applied to the corona-wire electrode to produce a corona discharge and the produced unipolar ions moved toward the inner cylinder due to the high electric field in the space. The inner cylinder section was made out of a perforated cylindrical tube with holes of 2.5 mm in diameter in order to allow ions to flow in the charging zone. The width of the mesh screen opening on the inner cylinder was about 20 mm. The mesh screen voltage applied on the inner cylinder driven the ions through the mesh screen openings on the inner cylinder to the charging zone, while the outer cylinder was connected to the electrical ground. This mesh screen voltage could regulate the ion current flow through the mesh screen. The fraction of ions drawn into the charging zone was equal to the ratio of the electric field strengths on either side of the mesh screen opening. In the charging zone, the aerosol particles impacted with the unipolar ions and were charged electrically.

The ion concentration, N_i, in the charging zone of the charger as a function of the ion current, I_{ch}, could be

Table 1 Comparison of different corona aerosol chargers.

Reference	Inner Electrode Diameter	Outer Electrode Diameter	Charging Zone length	Aerosol Flow Rate	Sheath Air Flow Rate	Corona Voltage Range
Liu *et al.* [4]	n/a	n/a	n/a	n/a	No	n/a
Pui [5]	25 µm	16.7 mm	9.53 mm	4 L/min	1 L/min	n/a
Buscher *et al.* [6]	n/a	30 mm	11.7 mm	2 L/min	0.5 L/min	4.5 kV
Kruis and Fissan [7]	25 µm	16 mm	150 mm	n/a	No	n/a
Biskos *et al.* [8]	16 µm	74 mm	60 mm	5 L/min	No	2–9 kV
Intra [9]	300 µm	28 mm	25 mm	5 L/min	No	5–10 kV
Tsai *et al.* [10]	25 µm	n/a	26 mm	10 L/min	20 L/min	9 kV
Whitby [15]	n/a	n/a	n/a	70 L/min	No	0–9 kV
Medved *et al.* [16]	n/a	n/a	n/a	1.0 L/min	1.5 L/min	n/a
Hernandez-Sierra *et al.* [17]	3 mm	4 mm	55 mm	10 L/min	No	2.5–4 kV
Alonso *et al.* [18]	n/a	3.5 mm	25 mm	10 L/min	No	3.1–3.7 kV
Park *et al.* [19]	0.25 mm	n/a	n/a	5 L/min	5 L/min	3.5–5 kV
Qi *et al.* [20]	n/a	n/a	n/a	1 L/min	5 L/min	n/a
Intra and Tippayawong [21]	3 mm	4 mm	30 mm	5 L/min	No	3–5 kV
This Work	100 µm	17 mm	22 mm	1.5 L/min	No	6–8 kV

n/a: information not available.

Table 2 Limits of the investigated variables.

Variable	Range
Corona-wire diameter	100 µm
Inner cylinder diameter	30 mm
Outer cylinder diameter	60 mm
Corona-wire voltage	5.0 to 8.0 kV
Mesh screen voltage	100, 300 V
Ions generated	Positive ion
Ionized gas	Air
Aerosol flow rate	1.5 L/min
Pressure	1 bar
Temperature	30 °C

calculated by the following equation [9],

$$N_i = \frac{I \ln(r_2 / r_1)}{2\pi LeVZ_i} \quad (1)$$

where r_1 and r_2 are the radii of the inner and outer cylinders, L is the width of the mesh screen opening on the inner cylinder, e is the value of elementary charge on an electron, V is the applied corona voltage on the inner cylinder, and Z_i is the ion electrical mobility, 1.15×10^{-4} m^2/Vs for positive ion [23]. In the unipolar charging studies, it is require to know the charging parameter, $N_i t$, where t is the particle charging time, and could be estimated from the equation,

$$t = \frac{(r_2^2 - r_1^2)L}{Q_a} \quad (2)$$

where Q_a is the aerosol flow rate.

3 Experimental Setup

3.1 Current-Voltage Characteristics

The experimental setup for investigating the current-voltage characteristics of the studied charger was consisted of a tested charger, an adjustable DC high voltage power supply and an electrometer. As shown in Table 2, the positive DC high voltage of about 5.0 to 8.0 kV was applied to the corona-wire electrode of the charger with an adjustable commercial DC high voltage power supply (Model 602C-100P, Spellman High Voltage Electronics Corporation, Blvd Hauppauge, NY, USA). A second adjustable commercial DC high voltage power supply (Model 602C-100P, Spellman High Voltage Electronics Corporation, Blvd Hauppauge, NY, USA) was used to maintain the mesh screen voltage difference on the inner cylinder in the range from 100 to 300 V. This was needed to evaluate the penetration of ions through the mesh screen openings on the inner cylinder into the charging zone. The ion currents in the charging zone of the tested charger were directly measured with an electrometer (model 6517A, Keithley Instruments, Inc., Cleveland, OH, USA) via the electrical grounded outer cylinder.

3.2 Charging Efficiency and Particle Losses Determinations

The schematic of the experimental setup for investigating the particle charging efficiencies and particle losses in the studied charger is shown in Fig. 2. There were four indices used for investigating the charger's charging performance. These were the intrinsic charging efficiency (η_{in}), the extrinsic charging efficiency (η_{ex}), the electrostatic loss (L_{el}), and the diffusion loss (L_d). Fig. 2(a) shows the experimental

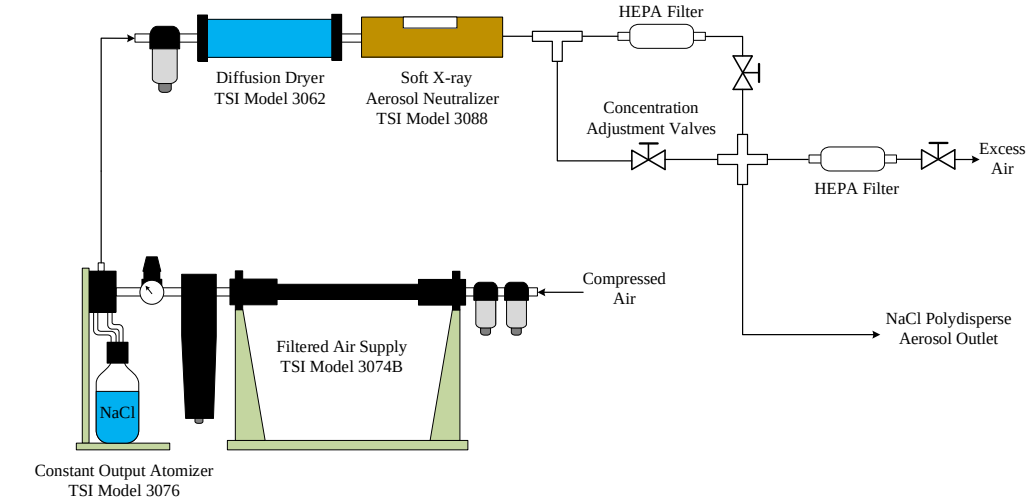

(a)

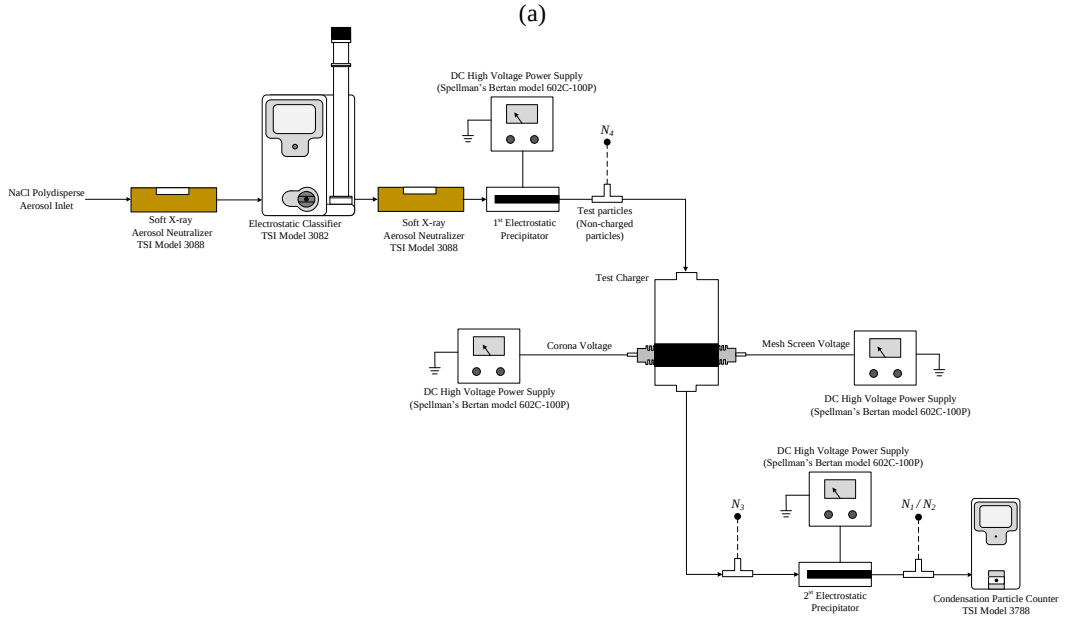

(b)

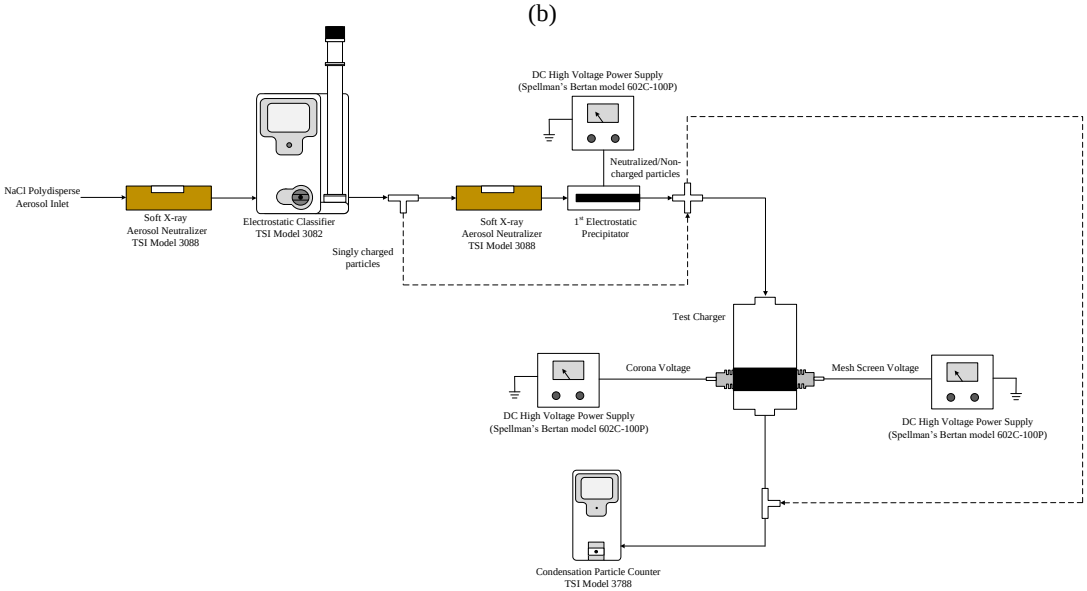

(c)

Fig. 2 Experimental setups a) for the generation of test NaCl polydisperse aerosol, b) for the measurement of intrinsic and extrinsic charging efficiencies, and c) for the measurement of particle loss of the charger.

setup for the generation of test NaCl polydisperse aerosol. The experimental setup consisted of an atomizer aerosol generator, a filtered air supply, an aerosol neutralizer, a concentration adjustment valves, a HEPA filter and a diffusion dryer. In this study, sodium chloride (NaCl) polydisperse aerosol was produced by nebulizing a NaCl solution (w/w 0.1 % in water) with an atomizer aerosol generator (Model 3076, TSI Inc., St. Paul, MN, USA) and a filtered air supply (Model 3074B, TSI Inc., St. Paul, MN, USA). The polydisperse aerosol particles coming out of the atomizer aerosol generator were still wet and were then dried to relative humidity less than about 30 % RH in the diffusion dryer (Model 3062, TSI Inc., St. Paul, MN, USA). The generated polydisperse aerosol have some level of electric charge, some loss of particles due to the electrostatic charges in the system may have been evident. To avoid charged particles tend to deposit on tube walls and other surfaces, the soft X-ray aerosol neutralizer (Model 3088, TSI Inc., St. Paul, MN, USA) was used to neutralize the aerosol and to bring the aerosol particles to the Boltzman charge equilibrium. In this system, the particle number concentration can be adjusted by the concentration adjustment valves and a HEPA capsule filter (Model 1602051, TSI Inc., St. Paul, MN, USA). The mean diameter, number concentration and geometric standard deviation of the generated particles were about 59.8 nm, 4.54×10^5 particles/cm^3 and 2.0, respectively, as shown in Fig. 3.

Fig. 2(b) shows the experimental setup for the intrinsic and extrinsic charging efficiency measurements of the tested charger. The experimental setup consisted of a tested charger, an adjustable DC high voltage power supply, an aerosol neutralizer, an electrostatic precipitator (ESP), an electrostatic classifier, and an ultrafine condensation particle counter (UCPC). In this study, NaCl polydisperse particles were then classified according to their electrical mobility using a soft X-ray aerosol neutralizer and an electrostatic classifier (Model 3082, TSI Inc., St. Paul, MN, USA) with a long-differential mobility analyzer, long DMA (model 3081, TSI Inc., St. Paul, MN, USA) with sheath air flow of about 3.0 L/min allowing for a mobility diameter selection from 15 to 670 nm. The particles exiting the classifier at a given voltage were nearly singly charged monodisperse particles. The fraction of multiply charged large particles exiting the classifier was minimized to about 10% or less for all particles size in the range between 20 nm and 300 nm by having the particle size distribution of the test aerosol centered on a mode diameter of about 30 nm. To remove entirely the charged particles, the singly charged monodisperse particles then entered the second soft X-ray aerosol neutralizer and the first ESP with an applied DC high voltage of about 3.5 kV using a DC high voltage power supply. Downstream from the ESP the uncharged monodisperse test particles were produced. Only uncharged particles were entered the tested charger.

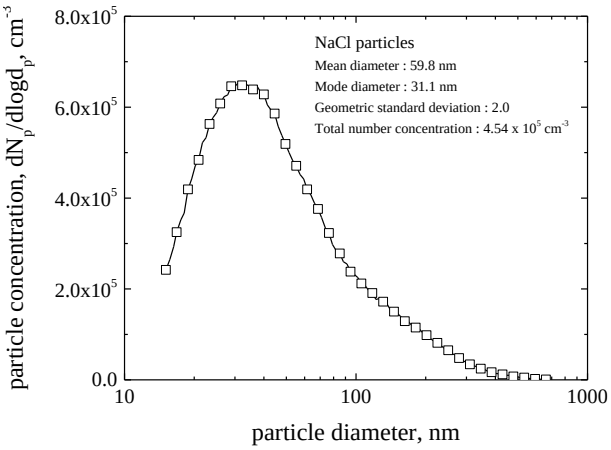

Fig. 3 Nanoparticle concentration and size distribution of sodium chloride particles generated from an atomizer.

After the charged aerosol flow exited the charger, it passed through the second ESP. To measure the particle concentration downstream of the tested charger, further on, the charged aerosol flow was entered an UCPC (Model 3788, TSI Inc., St. Paul, MN, USA). In this work, the intrinsic and extrinsic charging efficiencies of the charger were measured at the aerosol flow rate of about 1.5 L/min. The intrinsic charging efficiency can be calculated by [24]:

$$\eta_{in} = 1 - \frac{N_1}{N_2} \tag{3}$$

where N_1 and N_2 are the particle concentration downstream of the second ESP when both the charger and the applied voltage to the second ESP were ON or OFF, respectively. The extrinsic charging efficiency, which is the parameter of interest in a practical application, was defined as the fraction of particles exiting outside the charger that carried at least a unit of charge, and could be calculated by [24]:

$$\eta_{ex} = \frac{N_3 - N_1 / T}{N_4} \tag{4}$$

where N_3 is the particle concentration downstream of the tested charger when the charger voltage is ON, N_4 is the particle concentration upstream of the tested charger and T is the transmission efficiency of neutral particles passing through the second ESP.

Fig. 2(c) shows the experimental setup for the measurement of loss of singly charged, neutralized and non-charged particles in the charger. The experimental setup consisted of a tested charger, an adjustable DC high voltage power supply, an aerosol neutralizer, an ESP, an electrostatic classifier, and an UCPC. In this work, both electrostatic and diffusion losses and penetration of particles in the tested charger were measured at an aerosol flow rate of about 1.5 L/min. The particles exiting the classifier were nearly singly charged monodisperse particles at a given voltage. The

singly charged particles were used as a test aerosol. For non-charged and neutralized particles, these particles were entered a soft X-ray aerosol neutralizer, followed by an ESP to which a DC high voltage of about 3.5 kV is applied. With the high voltage on the ESP is ON and OFF, non-charged and neutralized particles can be produced, respectively. Singly charged, neutralized and non-charged monodisperse particles were then entered the tested charger. The electrostatic loss, L_{el}, and diffusion loss, L_d, of particles in the charger could be obtained from the following equations [18]:

$$L_{el} = \frac{N_{out,\,\mathrm{OFF}} - N_{out,\,\mathrm{ON}}}{N_{in}} \tag{5}$$

$$L_d = 1 - \frac{N_{out,\,\mathrm{OFF}}}{N_{in}} \tag{6}$$

where N_{in} is the particle concentrations were measured upstream of the charger, $N_{out,\,\mathrm{OFF}}$ is the particle concentrations were measured downstream of the charger when no voltage is applied on the charger, and $N_{out,\,\mathrm{ON}}$ is the particle concentrations were measured downstream of the charger when voltage is applied on the charger.

4 Results and Discussion

Fig. 4 shows the variations in ion current and ion concentration in the charging zone of the studied charger with a given corona voltage. Both ion current and ion concentration in the charging zone increased monotonically with increasing corona voltage. As shown in Fig. 4, the onset of corona voltages were 5.0 and 5.5 kV at an ion currents of 3.20×10^{-10} and 2.90×10^{-10} A for the mesh screen voltage of 100 and 300 V, respectively. As a result, there is a penetration of ions through the mesh screen opening on the inner cylinder into the charging zone. When the corona voltage increased from 5.5 to 8.0 kV, at the mesh screen voltage of 100 V, the ion current would increase from 2.90×10^{-10} to 3.66×10^{-8} A and the ion concentration would increase from 7.50×10^{9} and 5.92×10^{11} ions/m^3.

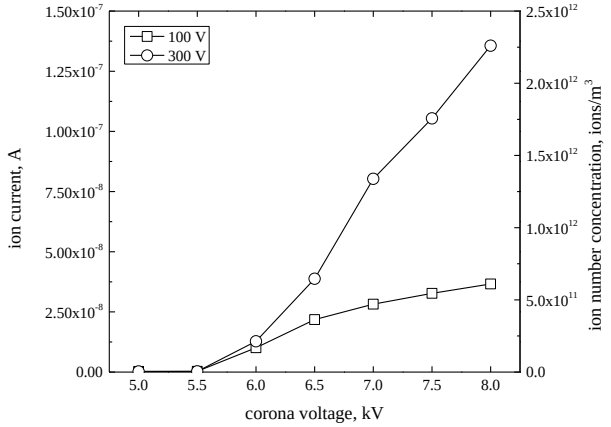

Fig. 4 Variations in ion current and ion concentration with corona voltage of the studied charger.

corona voltage in the range between 6.0 kV and 8.0 kV.

Fig. 5 shows the variations in N_it product with corona voltage of the studied charger at the aerosol flow rate of 1.5 L/min. In this study, the particle charging time of the charger was 0.54 sec when the aerosol flow rate was 1.5 L/min. It was shown that the N_it product of the charger increased with increasing the applied corona and mesh screen voltages because the N_it product was product of the ion concentration (n_i) and the particle charging time (t) and was controlled by the corona voltage and the aerosol flow rate. That is to say, increasing corona and mesh screen voltages could lead to a higher ion concentration inside the charging zone of the charger. It results in the possibility of an increasing intrinsic charging efficiency of the charger. As shown in Fig. 5, the N_it products increase from 4.06×10^{9} to 3.20×10^{11} ions/m^3.s and 3.68×10^{9} to 1.18×10^{12} ions/m^3.s when the corona voltage increases from 5.5 to 8.0 kV at a mesh screen voltage between 100 and 300 V, respectively.

The intrinsic particle charging efficiency was important for optimizing the charger performance and to find out the optimal operating condition of the charger. Fig. 6 shows the intrinsic charging efficiency of the charger as a function of particle diameters in the range between about 50 nm and 500 nm for various applied corona and ion driving voltages at the aerosol flow rate of 1.5 L/min. Results show that the intrinsic charging efficiencies increase with increasing the corona and mesh screen voltages at a given particle size. At a given corona voltage, the intrinsic charging efficiency of particle reached a constant of about 99% for particles in the size range between 50 and 200 nm and decrease with particle sizes in the range of about 300 to 500 nm.

Fig. 7 shows the extrinsic particle charging efficiency of the charger as a function of particle sizes in the range of about 50 to 500 nm at various corona voltages and mesh screen voltages. The test aerosol flow rate was fixed at 1.5 L/min. It should be noted that the intrinsic particle charging efficiency is different from the

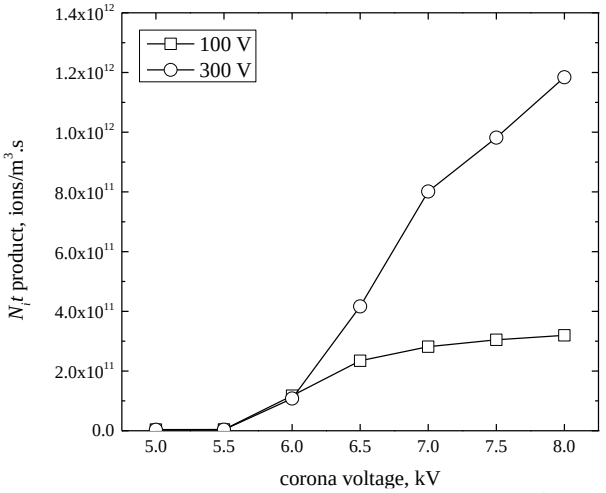

Fig. 5 Variations in N_it product with corona voltage of the studied charger.

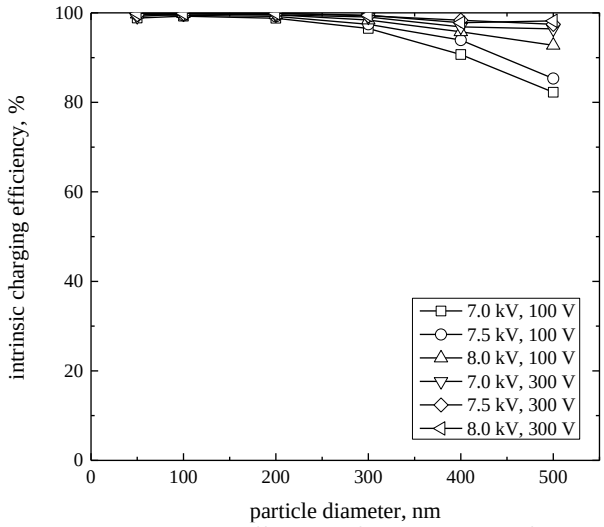

Fig. 6 Intrinsic charging efficiency of the charger as a function of particle diameter at different operating applied corona and mesh screen voltages.

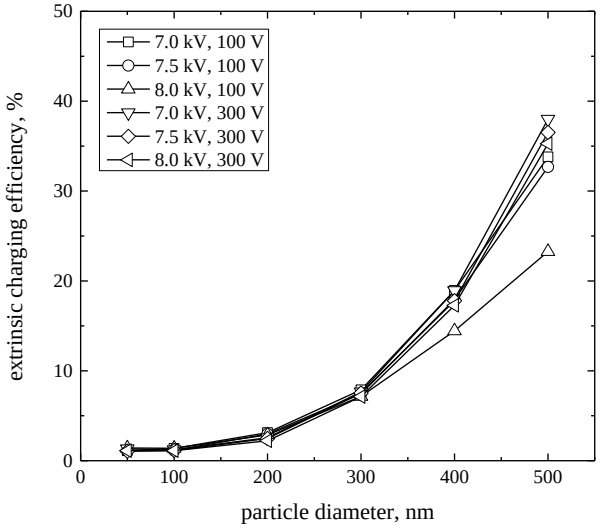

Fig. 7 Extrinsic charging efficiency of the charger as a function of particle diameter at different operating applied corona and mesh screen voltages.

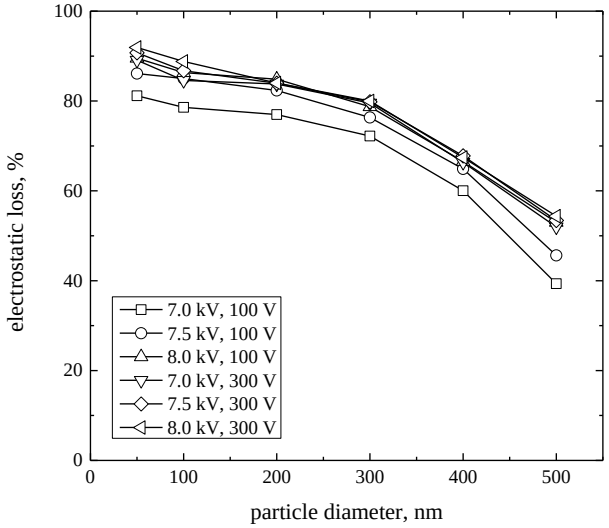

Fig. 8 Electrostatic loss of particle in the charger as a function of particle diameter at different operating applied corona and mesh screen voltages.

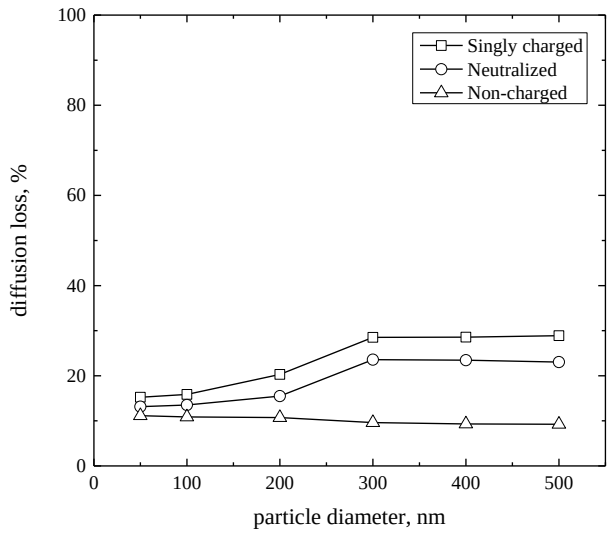

Fig. 9 Diffusion loss of singly charged, neutralized and non-charged particles in the charger as a function of particle diameter.

extrinsic particle charging efficiency because the latter takes into account the charged particle losses in the charger. It was found that the extrinsic particle charging efficiency increased with increasing particle size and decreased as the applied corona voltage increased. The extrinsic particle charging efficiency increased as the mesh screen voltage increased at a given corona voltage. In addition, the higher extrinsic particle charging efficiency could be derived with a sufficiently high corona voltage at the appropriate mesh screen voltage and aerosol flow rate. The best extrinsic particle charging efficiency was about 1.32 to 38% for particle sizes in the range between 50 nm and 500 nm. It occurred at corona voltage and mesh screen voltages of about 7.0 kV and 300 V, respectively.

Fig. 8 shows the electrostatic loss of particles in the charging zone as a function of particle diameters in the size range between 50 nm and 500 nm for various applied corona and mesh screen voltages at an aerosol flow rate of about 1.5 L/min. Larger particles were found to have lower electrostatic loss at the given applied corona and mesh screen voltages. The electrostatic loss of particles in the charging zone increased as the applied corona and mesh screen voltages increased. It should be noted that the electrostatic loss of particles depended on how many particles could achieve a charge, which increased with particle diameter and the electrical migration velocity or mobility of the charged particles, which decreased with particle diameter. The highest electrostatic loss of particles in the charging zone was observed for particles with diameters of about 50 nm. It was about 89.08, 90.73 and 91.91% at a mesh screen voltage of about 300 V for corona voltages of 7.0, 7.5 and 8.0 kV, respectively.

Fig. 9 shows the diffusion loss of singly charged,

neutralized and non-charged particles in the charging zone of the charger as a function of particle diameter. In case of the singly charged and neutralized particles, larger particles were found to have higher losses due to Brownian diffusion and space charge effects than smaller particles. For the non-charged particle, smaller particles were found to have higher losses due to Brownian diffusion motion and space charge effect than larger particles. The highest diffusion loss was seen to be about 28.88, 23.03 and 11.15% for singly charged, neutralized and non-charged particles with diameter of 500, 500 and 50 nm, respectively.

5 Conclusion

A cylindrical tri-axial charger for charging aerosol particles by unipolar ions was designed, constructed, and evaluated for the corona discharge characteristics, the intrinsic and extrinsic particle charging efficiencies and the particle losses. Current-voltage characteristics were determined. Ion concentration and $N_i t$ product with particle diameter were established. The charging performance of the studied charger was determined for particle sizes in the range between 50 nm and 500 nm under different operating conditions that included corona voltage of about 7.0 to 8.0 kV, mesh screen voltage of about 100 to 300 V and aerosol flow rate of about 1.5 L/min. It was found that the corona discharge current increased from 2.90×10^{-10} to 3.66×10^{-8} A and 2.40×10^{-10} to 1.36×10^{-7} A and the ion concentration increased from 7.50×10^{9} ions/m^3 and 5.92×10^{11} ions/m^3 and 6.21×10^{9} and 2.19×10^{12} ions/m^3 when the corona voltage increased from 5.5 to 8.0 kV for the mesh screen voltage between 100 and 300 V, respectively. The intrinsic particle charging efficiency reached a constant of about 99% for particle sizes in the range between 50 and 200 nm and decreased with particle sizes in the range between about 300 nm to 500 nm at a given corona voltage. The best extrinsic particle charging efficiency of the studied charger seemed to occur at corona voltage and mesh screen voltage of about 7.0 kV and 300 V, and was about 1.32 to 38 % for particle sizes in the range from 50 to 500 nm. The highest electrostatic loss of particles was observed for particle diameter of about 50 nm. It was about 89.08, 90.73 and 91.91% at a mesh screen voltage of about 300 V for the corona voltages of 7.0, 7.5 and 8.0 kV, respectively. Finally, the highest diffusion loss was about 28.88, 23.03 and 11.15% for singly charged, neutralized and non-charged particles in diameter of 500, 500 and 50 nm, respectively.

Acknowledgements

The authors gratefully acknowledge the Electricity Generating Authority of Thailand (EGAT), Research contract no. GGR010100089000. The authors wish to thank Prof. Dr. Rainer Zawadzki of Central New Mexico Community College for the valuable contribution during the preparation of the manuscript.

References

[1] H. J. White, *Industrial Electrostatic Precipitation*. Addison-Wesley, Reading, Massachusetts, 1963.

[2] P. Intra and N. Tippayawong, "Progress in unipolar corona discharger designs for airborne particle charging: A literature review," *Journal of Electrostatics*, Vol. 67, No. 4, pp. 605–615, 2009.

[3] P. Intra and N. Tippayawong, "An overview of differential mobility analyzers for size classification of nanometer-sized aerosol particles," *Songklanakarin Journal of Science and Technology*, Vol. 30, No. 2, pp. 243–256, 2008.

[4] B. Y. H. Liu, K. T. Whitby and H. H. S. Yu, "Diffusion charging of aerosol particles at low pressures," *Journal of Applied Physics*, Vol. 38, No. 4, pp. 1592–1597, 1967.

[5] D. Y. H. Pui, "Experimental study of diffusion charging of aerosols," *Ph.D. Thesis*, University of Minnesota, Minneapolis, MN, USA, 1976.

[6] P. Büscher, A. Schmidt-Ott, and A. Wiedensohler, "Performance of a unipolar "Square Wave" diffusion charger with variable nt-product," *Journal of Aerosol Science*, Vol. 25, No. 4, pp. 651–663, 1980.

[7] F. E. Kruis and H. Fissan, "Nanoparticle charging in a twin Hewitt charger," *Journal of Nanoparticle Research*, Vol. 3, pp. 39–50, 2001.

[8] G. Biskos, K. Reavell, and N. Collings, "Electrostatic characterization of corona-wire aerosol charges," *Journal of Electrostatics*, Vol. 63, pp. 69 – 82, 2005.

[9] P. Intra, "Corona discharge in a cylindrical triode charger for unipolar diffusion aerosol charging," *Journal of Electrostatics*, Vol. 70, No. 1, pp. 136–143, 2012.

[10] C. J. Tsai, G. Y. Lin, H. L. Chen, C. H. Huang, and M. Alonso, "Enhancement of extrinsic charging efficiency of a nanoparticle charger with multiple discharging wires," *Aerosol Science and Technology*, Vol. 44, No. 10, pp. 807–816, 2010.

[11] C. L. Chien, C. J. Tsai, H. L. Chen, G. Y. Lin, and J. S. Wu, "Modeling and validation of nanoparticle charging efficiency of a single-wire corona unipolar charger," *Aerosol Science and Technology*, Vol. 45, No. 12, pp. 1468–1479, 2011.

[12] C. L. Chien and C. J. Tsai, "Improvement of the nanoparticle charging efficiency of a single-wire corona unipolar charger by using radial sheath airflow: Numerical study," *Aerosol Science and Technology*, Vol. 47, No. 4, pp. 417–426, 2013.

[13] P. Intra, A. Yawootti and N. Tippayawong, "Electrostatic evaluation of a unipolar diffusion and field charger of aerosol particles by a corona discharge," *Particulate Science and Technology*, Vol. 31, No. 6, pp. 621–631, 2013.

[14] P. Intra, A. Yawootti, and P. Rattanadecho, "Influence of the corona-wire diameter and length on corona discharge characteristics of a cylindrical tri-axial charger," *Journal of Electrostatics*, Vol. 74, No. 1, pp. 37–46, 2015.

[15] K. T. Whitby, "Generator for producing high concentration of small ions," *Review of Scientific Instruments*, Vol. 32, No. 12, pp. 1351–1355, 1961.

[16] A. Medved, F. Dorman, S. L. Kaufman, and A. Pocher, "A new corona-based charger for aerosol particles," *Journal of Aerosol Science*, Vol. 31, pp. s616–s617, 2000.

[17] A. Hernandez-Sierra, F. J. Alguacil, and M. Alonso, "Unipolar charging of nanometer aerosol particle in a corona ionizer," *Journal of Aerosol Science*, Vol. 34, pp. 733–745, 2003.

[18] M. Alonso, M. I. Martin, and F. J. Alguacil, "The measurement of charging efficiencies and losses of aerosol nanoparticles in a corona charger," *Journal of Electrostatics*, Vol. 64, pp. 203–214, 2006.

[19] D. Park, M. An, and J. Hwang, "Development and performance test of a unipolar diffusion charger for real-time measurements of submicron aerosol particles having a log-normal size distribution," *Journal of Aerosol Science*, Vol. 38, No. 4, pp. 420–430, 2007.

[20] C. Qi, D. R. Chen, and D. Y. H. Pui, "Experimental study of a new corona-based unipolar aerosol charger," *Journal of Aerosol Science*, Vol. 38, No. 7, pp. 775–792, 2007.

[21] P. Intra and N. Tippayawong, "Effect of needle cone angle and air flow rate on electrostatic discharge characteristics of a corona-needle ionizer," *Journal of Electrostatics*, Vol. 68, No. 3, pp. 254–260, 2010.

[22] P. Intra and N. Tippayawong, "Design and evaluation of a high concentration, high penetration unipolar corona ionizer for electrostatic discharge and aerosol charging," *Journal of Electrical Engineering and Technology*, Vol. 8, No. 5, pp. 1175–1181, 2013.

[23] P. Intra, A. Yawootti, and P. Rattanadecho, "Corona discharge characteristics and particle losses in a unipolar corona-needle charger obtained through numerical and experimental studies," *Journal of Electrical Engineering and Technology*, Vol. 12, No. 5, 2021–2030, 2018.

[24] G. P. Reischl, J. M. Makela, R. Harch, and J. Necid, "Bipolar charging of ultrafine particles in the size range below 10 nm," *Journal of Aerosol Science*, Vol. 27, No. 6, pp. 931–939, 1996.

[25] F. X. Ouf and P. Sillon, "Charging efficiency of the Electrical Low Pressure Impactor's corona charger: Influence of the fractal morphology of nanoparticle aggregates and uncertainty analysis of experimental results," *Aerosol Science and Technology*, Vol. 43, No. 7, pp. 685–698, 2009.

P. Intra received the BS.Tech.Ed. degree in Electrical Engineering from Rajamangala University of Technology Lanna, Thailand in 2001, the M.Eng. in Energy Engineering and Ph.D. degree in Mechanical Engineering from Chiang Mai University, Thailand in 2003 and 2006, respectively. He is currently an Associate Professor in the College of Integrated Science and Technology, Rajamangala University of Technology Lanna, Thailand. He does research in aerosol electrical mobility analysis, corona discharge-based aerosol charging, electrostatic precipitation and pulsed electric field and electroporation.

P. Wanusbodeepaisarn received High Voc. Cert. in Electrical and Electronic from Rajamangala University of Technology Krungthep, Thailand in 1984. He is currently a CEO in Pico Innovation Co., Ltd. He does research in aerosol and particle measurement.

T. Siri-achawawath received B.Eng. degree in Electrical Engineering from King Mongkut's University of Technology North Bangkok, Thailand in 2000. He is currently a CEO in Innovative Instrument Co., Ltd. He does research in aerosol and particle measurement.